Fault Tolerance Analysis and Measurement of a Spatial Power Amplifier

Sean Ortiz, Mete Ozkar, Alexander Yakovlev*, Michael Steer, and Amir Mortazawi

North Carolina State University, Department of Electrical and Computer Engineering, Raleigh, NC 27695

*University of Mississippi, Department of Electrical Engineering, University, MS 38677.

Abstract — **The performance degradation due to device failures in a spatial power combining system is presented in this paper, including analysis and measurement. For this study, a 5x5 amplifier array, employing 17 dBm (P1dB) MMIC amplifiers, has been designed and tested. Individual unit cells have been turned off in order to represent a system with device failures. Results for both simulated and measured array performance versus device failures are given.**

I. INTRODUCTION

Spatial power combining amplifier arrays have shown great promise in the past few years with systems producing noteworthy power levels, power added efficiencies, and power combining efficiencies from an array of solid-state devices [1]-[3]. Arrays in varying configurations have been designed by various authors, including arrays based on grids, CPW-fed slot antennas, microstrip patch antennas, dielectric slabs, and tapered slotlines [1-11]. Each of these systems utilizes various radiating elements or transmission mediums, but they all divide/combine power by using an array of radiators to receive/radiate a signal from/to a single source/receiver. By doing so, losses are reduced by eliminating the need for transmission line based power dividers (Wilkinson, Lange, etc.). Furthermore, spatial power combining amplifiers are expected to be more fault tolerant when compared to traveling wave tube amplifiers, due to the large number of devices used in parallel. They may also be less costly to fabricate, due to their use of semiconductor technologies, which have shown lower and lower production costs in past years. This fault tolerant behavior will be the focus of this paper.

In order to study the degradation in amplifier performance versus device failure, an existing perpendicularly-fed patch array [6] was modified to allow for the complete control of the individual amplifiers (turning on or off individual devices). A conceptual drawing of this array is shown in Fig. 1. In this figure, an array of microstrip patch antennas receive a signal of uniform amplitude and phase from a hard horn feed on the left. The signal is then coupled to microstrip lines within the array where it is amplified. It is then coupled to the microstrip patch antennas on the right and radiated into free space. In this design, the amplifying and biasing circuitry are located in the space behind the antennas, making it simple to bias the individual amplifiers. Using such a structure, the power collected either in the far-field with a standard gain horn or with a hard horn feed could be measured versus the number of active amplifiers. In addition, this system has been modeled in a previous work [11]; thereby allowing a comparison between simulated and measured data to be made.

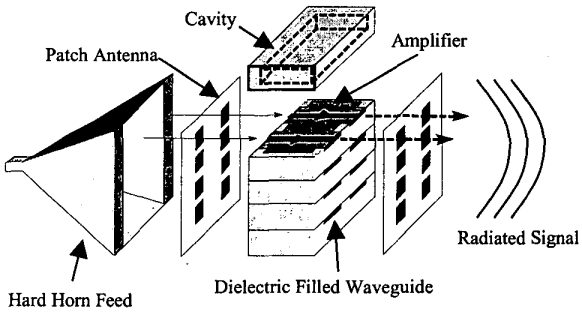

Fig. 1. A conceptual drawing of the perpendicularly-fed patch array fed by a hard horn and radiating into free space.

II. DESIGN

The development of the 5x5 perpendicularly-fed patch array was documented in a previous work [6]. A brief description of this structure will be given with an emphasis on the changes made to facilitate the individual biasing of the devices. Each unit cell shown in Fig. 1 consists of a receiving antenna coupled to a microstrip line, an amplifier, and a transmitting antenna. The microstrip patch antennas on the left of the diagram are coupled to a slot aperture, which then feeds a dielectric filled waveguide. The dielectric filled waveguide is then coupled to a microstrip line, which in turn feeds the amplifying element. The same transition from the

803-6538-0/01/$10.00 © 2001 IEEE

microstrip line to the patch antenna is used for the radiating antenna on the right side of the diagram. The array is formed from stacking the trays vertically, which also forms the dielectric filled waveguide (top wall from the upper tray and bottom and side walls from the bottom tray). This perpendicularly-fed patch array is then fed using a hard horn feed to distribute the power equally among the individual unit cells [13].

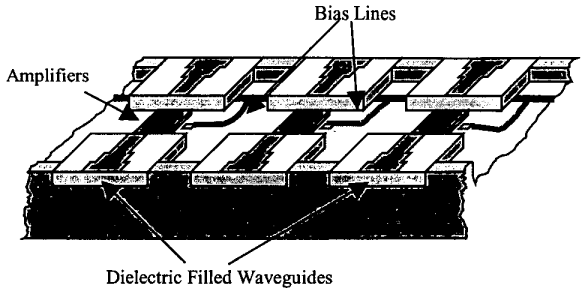

Fig. 2. A conceptual drawing of the perpendicularly-fed patch array unit cells illustrating the bias line placement.

The microstrip patch antenna feed was designed as described in the previous work [6] and simulated using *Agilent HFSS™*. A *Rogers TMM3™* substrate with ε_r=3.27 and thickness of 0.381 mm was chosen for both the microstrip lines and the microstrip patch antennas. Since this gives a different impedance from that of the waveguide, an impedance transformer was added to mach the waveguide to the 50 Ω microstrip line. The antenna dimensions were then calculated (length of 7.4 mm and width of 8.1 mm), as well as the slot (length of 4.8 mm and height of 0.381 mm). For amplification, a self-biasing, PHEMT, GaAs MMIC amplifier (*Filtronic LMA411™*) with 18 dB gain and 17 dBm output power at 1 dB compression was chosen. The biasing arrangement can be seen in Fig. 2, which illustrates the unit cell layout. Each bias line (magnet wire) passes beneath the ground plane of the microstrip lines feeding the amplifiers. In this way, each amplifier has a separate bias line and can be individually controlled. Finally, the unit cell spacing is identical to the previously published results (i.e. 15.24 mm).

A complete simulation of the perpendicularly-fed patch array with hard horn feeds was performed. Electromagnetic modeling of the entire spatial power combining amplifier is based on the decomposition of the system into modules, including hard horn (feeding/collecting), N-port perpendicularly-fed patch array to waveguide transitions, waveguide-microstrip line junctions, and amplifier circuits [12]. A full-wave integral equation formulation was developed for the electromagnetic modeling of the waveguide to aperture-coupled patch array, resulting in the GSM of the 25 dielectric filled waveguides to the hard horn feed. The GSM for the hard horn feed was obtained using the mode-matching technique [13]. All the modules within the power combining system including the amplifier network could then be cascaded to find the overall response of the system. The cascading can be performed within a nonlinear circuit simulator such as *Agilent ADS™* in order to use nonlinear models for the amplifiers.

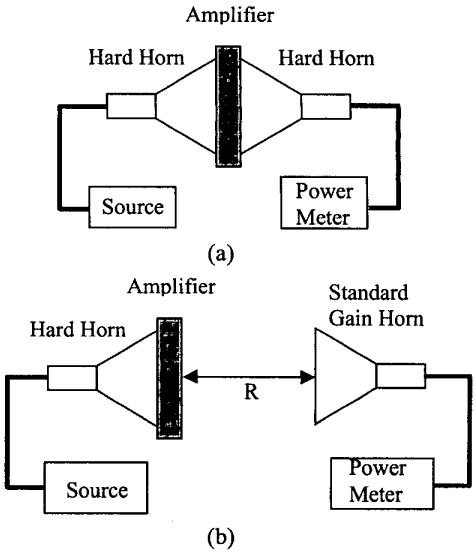

Fig. 3. Measurement setup for the spatial amplifier array. (a) Closed system setup. (b) Far-field system setup: $R > 2D^2/\lambda o$.

III. RESULTS

Two experiments were performed to test the fault tolerant behavior of the spatial power combining amplifier array. The first experimental setup, shown in Fig. 3a, consists of a closed system containing the amplifier array with both feeding and collecting hard horns. In this experiment, the power compression curve of the amplifier array was measured for several cases, each consisting of different combinations of device failures. In each case, the frequency was set to 9.6 GHz, and the input power was swept from 0 to 25 dBm. It should be noted that under small signal excitation the amplifier array gave 16 dB of gain with 280 MHz of 3-dB bandwidth and a power combining efficiency of 50%. The power compression curves for several device failures (turned off) are shown in Fig. 4. In each case (1 cell, 2 cells, etc.), 5 random combinations of cells were chosen and measured with the exception of the 1 cell case. For this case, all 25 cells

were turned off one at a time. In addition, for each case the worst case performance (lowest gain) has been plotted. Simulated results for the same experiment are shown in Fig. 5. The amplifiers are modeled using the reported gain and compression characteristics of the MMIC, due to the lack of a nonlinear model. As can be seen when 20% of the active devices fail across the array, the measured array gain drops by approximately 2.7 dB while simulations predict 1.9 dB of drop in gain. It should be noted that the worst case cells are typically at the center of the array.

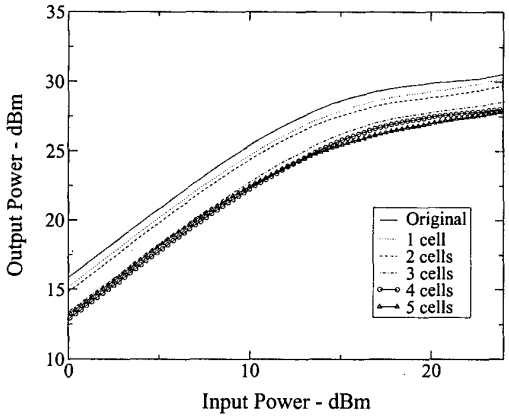

Fig. 4. Measured power compression curve of the amplifier array at 9.6 GHz with input and output hard horn feeds plotted for various numbers of device failures.

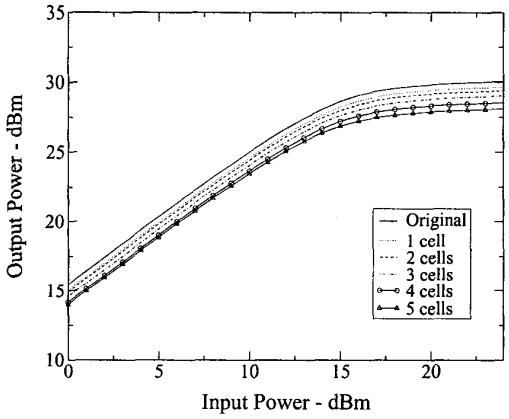

Fig. 5. Simulated power compression curve of the amplifier array at 9.6 GHz with input and output hard horn feeds plotted for various numbers of device failures.

For the second experiment, the effective transmitter power was determined [14] using the setup shown in Fig. 3b. The array was placed at a distance of 1 m from a standard gain horn having a gain of 16 dB at 9.6 GHz. The directivity of the array was calculated to be 17.8 dB using the formula given in [14] based on the array physical size. The same cells were then turned off as with the closed system. Fig. 6 shows the results for this experiment. It is interesting to see that the gain is slightly less than that of the closed. This may be due to an incorrect estimate of the array gain, which must be measured from the far-field radiation pattern for a more accurate result. In addition, the far-field radiation pattern of the array was calculated for the same device failures previously simulated. The antenna excitation (magnitude and phase) was extracted from the electromagnetic simulation for a case in which no collecting hard horn feed was present. In all cases, the main lobe of the radiation pattern is unaffected and only the sidelobe levels increase by several dB when 20% of the array elements are turned off.

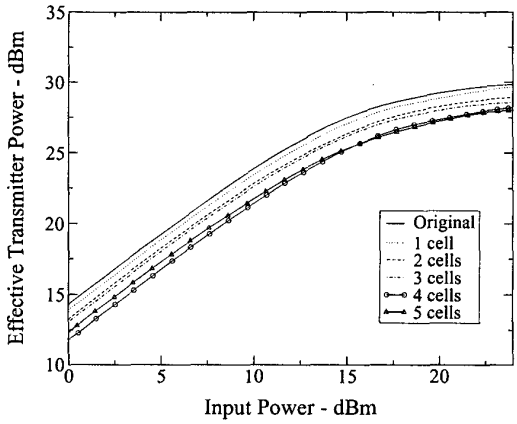

Fig. 6. Measured effective radiated power compression curve of the amplifier array at 9.6 GHz with an input hard horn feed plotted for various numbers of device failures.

IV. Conclusion

The performance degradation of a spatial power combining amplifier array versus device failure has been presented. In addition, both simulated and measured results were presented for several combinations of device failures. These results include collected and radiated power versus input power for up to 20% of the devices failed. In addition, E- and H-plane radiation patterns were also presented with up to 20% of the devices turned off. In conclusion, simulated and measured power compression curves compared reasonably well in predicting the system performance versus device failure (i.e. 36% loss in power for 20% of the devices failed).

ACKNOWLEDGEMENT

This work is supported by an Army Research Office – MURI grant under the Spatial and Quasi-Optical Power Combining DAAG-55-97-0132.

REFERENCES

[1] S. Ortiz, J. Hubert, L. Mirth, E. Schlecht, and A. Mortazawi, "A 25 watt and 50 watt Ka-band quasi-optical amplifier," *IEEE Int. Microwave Symp. Dig.*, pp. 797-800, June 2000.

[2] N. Cheng, T. Dao, M. Case, D. Rensch, and R. York, "A 60-watt X-band spatially combined solid-state amplifier," *IEEE Int. Microwave Symp. Dig.*, pp. 539-542, June 1999.

[3] J. Sowers, D. Pritchard, A. White, W. Kong, and O. Tang, "A 36 W, V-band, solid state source," *IEEE Int. Microwave Symp. Dig.*, pp. 235-238, June 1999.

[4] M. Kim, J. Rosenberg, R. P. Smith, R. M. Weikle, J. B. Hacker, M. P. De Lisio, and D. B. Rutledge, "A grid amplifier," *IEEE Microwave Guided Wave Lett.*, vol. 1, pp. 332-324, Nov. 1991.

[5] J. F. Hubert, J. Schoenberg, and Z. B. Popovic, "High-power hybrid quasi-optical Ka-band amplifier design," *IEEE Int. Microwave Symp. Dig.*, pp. 585-588, June 1995.

[6] S. Ortiz and A. Mortazawi, "A perpendicular aperture-fed patch array for quasi-optical power combining," *IEEE Int. Microwave Symp. Dig.*, pp. 667-670, June 1999.

[7] M. Kim, E. A. Soverro, J. B. Hacker, M. P. De Lisio, J.-C. Chiao, S.-J. Li, D. R. Cagnon, J. J. Rosenberg, and D. B. Rutledge, "A 100-element HBT grid amplifier," *IEEE Trans. Microwave Theory Tech.*, vol. 41, pp. 1762-1771, Oct. 1993.

[8] H. Hwang, T. W. Nuteson, M. B. Steer, J. W. Mink, J. Harvey, and A. Paolella, "A quasioptical dielectric slab combiner," *IEEE Microwave Guided Wave Lett.*, vol. 4, pp. 73-75, Feb. 1996.

[9] A. R. Perkons, and T. Itoh, "A 10-element active lens amplifier on a dielectric slab," *IEEE Int. Microwave Symp. Dig.*, pp. 1119-1121, June 1996.

[10] T. Ivanov, A. Balasubramaniyan, and A. Mortazawi, "One and two stage spatial amplifiers," *IEEE Trans. Microwave Theory Tech.*, vol 43, pp. 2138-2134, Sept. 1995.

[11] T. Ivanov and A. Mortazawi, "A two-stage spatial amplifier with hard horn feeds," *IEEE Microwave Guided Wave Lett.*, vol. 6, pp. 365-367, Feb. 1996.

[12] A. B. Yakovlev, S. Ortiz, M. Ozkar, A. Mortazawi, and M. B. Steer, "Electromagnetic modeling and experimental verification of a complete waveguide-based aperture coupled patch amplifier array," *IEEE Int. Microwave Symp. Dig.*, pp. 801-804, June 2000.

[13] M. A. Ali, S. Ortiz, T. Ivanov, and A. Mortazawi, "Analysis and measurement of hard horn feeds for the excitation of quasi-optical amplifiers," *IEEE Microwave Theory Tech.*, vol. 47, pp. 479-487, Apr. 1999.

[14] M. Gouker, "Toward standard figures-of-merit for spatial and quasi-optical power-combined arrays," *IEEE Trans. Microwave Theory Tech.*, vol. 43, pp. 1614-1617, Jul. 1995.

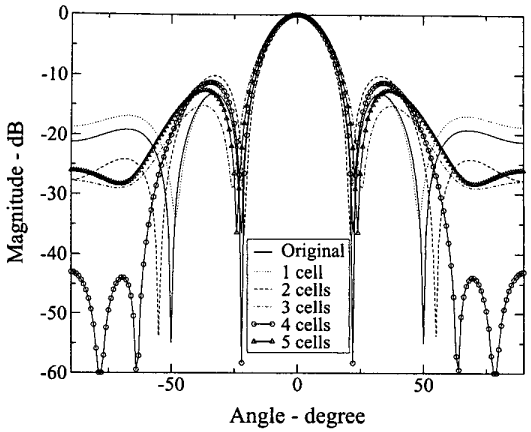

Fig. 7. Simulated E-plane radiation pattern of the amplifier array at 9.6 GHz with an input hard horn feed plotted for various numbers of device failures.

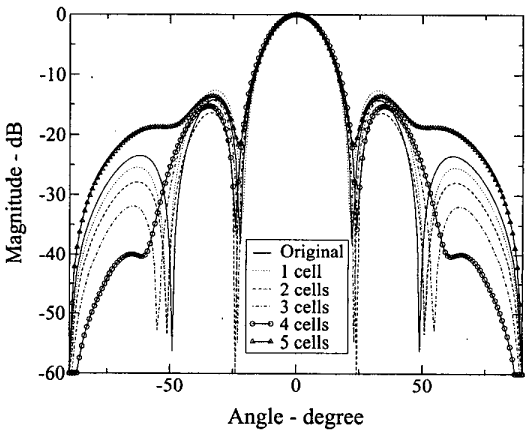

Fig. 8. Simulated H-plane radiation pattern of the amplifier array at 9.6 GHz with an input hard horn feed plotted for various numbers of device failures.